J. Phys. B: At. Mol. Opt. Phys. 25 (1992) 463–474. Printed in the UK

State-selective electron capture in slow collisions of C^{6+} and O^{6+} with He

J P M Beijers†, R Hoekstra†‡, A R Schlatmann†, R Morgenstern† and F J de Heer‡

† Kernfysisch Versneller Instituut, Zernikelaan 25, 9747 AA Groningen, The Netherlands
‡ FOM-Institute for Atomic and Molecular Physics, PO Box 41883, 1009 DB Amsterdam, The Netherlands

Received 11 September 1991

Abstract. State-selective capture and emission cross sections for single-electron capture in collisions of bare C^{6+} ions and He-like O^{6+} ions with helium are presented for impact velocities between 0.05 and 0.27 au ($62 \leq E(\text{eV amu}^{-1}) \leq 1852$). Experimental data have been obtained using VUV photon emission spectroscopy. They join previous higher energy measurements smoothly. Detailed comparisons are made with existing AO and MO close-coupling calculations. The entire data set is consistent with results concerning the influence of the projectile core on the capture process found in a theoretical study on collisions between multiply-charged ions and atomic hydrogen.

1. Introduction

The past few years have seen remarkable progress in our understanding of charge transfer in slow collisions ($v \leq 1$ au) between multiply-charged ions and neutral gas atoms. In fact, for single-electron capture (SEC) in (quasi) one-electron ion–atom collision systems recent, large scale close-coupling calculations generally reproduce the experimentally determined total- and state-selective cross sections over a large energy range (Fritsch and Lin 1991). While this detailed level of comparison is not (yet) feasible for multi-electron collision systems, (semi)classical models such as the classical overbarrier model and the Landau–Zener model do predict the major charge transfer channels surprisingly well (Niehaus 1986, Taulbjerg 1986).

A large amount of effort is presently being put into studying (quasi) two-electron ion–atom systems, e.g. multiply-charged ions colliding on He. In addition to SEC several two-electron processes can occur including double electron capture (DEC) and transfer excitation/ionization. These processes are studied experimentally via coincident energy gain spectroscopy (see e.g. Barat 1988) or electron spectroscopy (Mack 1987, Bordenave-Montesquieu *et al* 1987) and have yielded considerable insight into the mechanism of two-electron transfer. However, mostly SEC channels are dominantly populated and should be included in realistic treatments of these two-electron processes.

This paper presents new experimental results on emission- and state-selective SEC cross sections for the $O^{6+} + He$ and $C^{6+} + He$ collision systems. Because there are no other experimental data available, we have focused especially on the low impact velocity range between 0.05 and 0.27 au [$62 \leq E(\text{eV amu}^{-1}) \leq 1852$]. The reasons for choosing these particular collision systems are fourfold: (i) they are typical for (quasi)

0953-4075/92/020463+12$04.50

two-electron systems involving large projectile charges and the two-electron channels have been studied intensively (Mack and Niehaus 1987, Roncin *et al* 1989); (ii) state-of-the-art close-coupling calculations exist for these collision systems in the low energy regime (Kimura and Olson 1984, Fritsch and Lin 1986, Shimakura *et al* 1987); (iii) data on low energy collisions between low Z multiply-charged ions and neutral helium are relevant for plasma edge physics and impurity control in the poloidal divertor of the next generation large Tokamaks (Janev 1991); (iv) according to the classical overbarrier model, the ion core of the projectile does not directly affect the electron capture process (Niehaus 1986). However, in collisions with atomic hydrogen both experimental and theoretical investigations have shown a pronounced effect of the ion core on the total SEC cross section particularly at small impact velocities (Phaneuf *et al* 1982, Larsen and Taulbjerg 1984). More recently Harel and Jouin (1988) theoretically investigated the effect of the projectile core on the final l distributions in collisions between multiply-charged ions and atomic hydrogen. It is interesting to look for similar effects in SEC collisions with helium.

In collisions between O^{6+} and C^{6+} with He SEC processes preferentially populate the $3l$ states of the product ions which decay via VUV photon emission, see for example Gordeev *et al* (1983). We therefore use VUV photon spectroscopy to determine the relevant cross sections. Compared with energy gain spectroscopy, the technique of photon spectroscopy has the advantage of not being sensitive to angular scattering effects, which can become significant at low impact velocities. Our results extend the work reported by Dijkkamp *et al* (1985) to lower impact energies. Other experimental data include total SEC cross sections for the O^{6+}, C^{6+} + He systems from the Nagoya group (Iwai *et al* 1982, Okuno *et al* 1983) and photon emissiong cross sections at higher impact energies (>2 keV amu^{-1}) for O^{6+} + He by Liu *et al* (1989).

In the rest of the paper we will briefly describe the experimental apparatus and present and discuss our results in detail. Whenever possible we will compare our data with other experimental and theoretical work.

2. Experiment

The experiments were performed using a crossed-beam apparatus which will be briefly outlined here. The reader is referred to Hoekstra *et al* (1990) for further details. The projectile ions are extracted from an ECR ion source (Drentje 1985) at an extraction voltage of 4 kV and transported to the collision chamber with a system of bending and focusing magnets. For the C^{6+} projectile beam we use ^{13}CO in the ECR source in order to prevent contamination with He^{2+} and H_2^+. Before being crossed with an effusive helium beam the projectile ions are decelerated with a five-element electrostatic retardation lens to the desired energy and finally collected in a Faraday cup. The last element in the lens system encloses the collision region in order to define the collision energy unambigiously. The effective target pressure in the collision centre has been kept under 20 mPa in order to ensure single collision conditions. We use a 1 m radius grazing incidence VUV monochromator (10–80 nm) to observe the photon emission from the decaying $3l$ product states which are populated by the SEC processes. A position sensitive detector enables simultaneous detection of lines within a range of about 20 nm. The monochromator is positioned under the magic angle of 54.7° with respect to the ion-beam axis and tilted by 45° in order to cancel all polarization-dependent

effects. The collision chamber is surrounded by two pairs of Helmholtz coils to reduce the magnetic field strength perpendicular to the ion beam to less than a few μT.

The emission cross section $\sigma_{em}(\lambda)$ for a particular line follows from the measured signal $S(\lambda)$ (e.g. the area of the peak) via the relation

$$\sigma_{em}(\lambda) = \frac{4\pi}{\omega} \frac{q}{K(\lambda)Q} \frac{S(\lambda)}{NL} \tag{1}$$

where ω is the solid angle of observation, q the charge of the projectile ions, Q the accumulated ion charge, $K(\lambda)$ the quantum yield of the detection system, N the effective target density and L the observation length. Lifetime corrections are not necessary since all the observed product states decay within view of the detection system. The wavelength-dependent sensitivity of the optical detection system is calibrated absolutely by means of various ion and electron impact excitation processes with known cross sections. Details of the calibration procedure can be found in Kadota *et al* (1982) and Hoekstra (1990). The uncertainty in our cross section measurements comes from counting errors and target density fluctuations (statistical uncertainties) and from the sensitivity calibration of the VUV monochromator (systematic uncertainty). This systematic uncertainty is estimated to be 20%. Hoekstra *et al* (1990) report a detailed error discussion relevant for the present experiments.

With this setup we have measured the $3l \rightarrow 2l'$ and $4l \rightarrow 2l'$ lines emitted by the decaying O^{5+*} and C^{5+*} product ions. Equation (1) then yields the relevant emission cross sections. The results are described in the next section.

3. Results

3.1. O^{6+} + He

A typical VUV spectrum resulting from SEC in O^{6+} + He collisions is shown in figure 1. The following lines are observed: 3p→2s (15.0 nm), 3d→2p (17.3 nm), 3s→2p

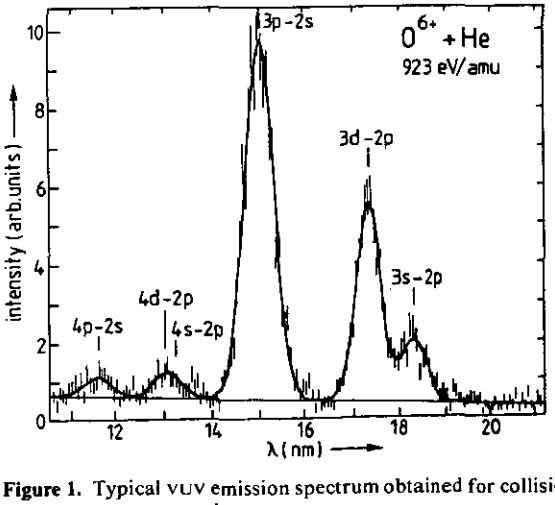

Figure 1. Typical VUV emission spectrum obtained for collisions of O^{6+} on He at an impact energy of 923 eV amu^{-1}.

Table 1. Experimental $3l$ and $n=3$ SEC cross sections with corresponding statistical errors (in units of 10^{-16} cm^2) for O^{6+} + He collisions.

E (keV amu^{-1})	σ(3s)	σ(3p)	σ(3d)	$\sigma(n=3)$
1.505	1.53 ± 0.15	6.69 ± 0.47	3.11 ± 0.24	11.3 ± 0.6
1.186	1.23 ± 0.15	6.66 ± 0.47	3.13 ± 0.24	11.0 ± 0.6
0.923	1.02 ± 0.12	5.93 ± 0.48	3.19 ± 0.29	10.1 ± 0.6
0.695	0.86 ± 0.10	5.34 ± 0.43	2.93 ± 0.27	9.12 ± 0.52
0.484	0.57 ± 0.09	4.89 ± 0.40	3.08 ± 0.28	8.54 ± 0.50
0.380	0.52 ± 0.08	4.32 ± 0.35	3.21 ± 0.29	8.05 ± 0.46
0.267	0.37 ± 0.08	3.55 ± 0.29	3.31 ± 0.30	7.23 ± 0.43
0.215	0.20 ± 0.07	2.86 ± 0.40	2.62 ± 0.35	5.69 ± 0.54
0.169	0.24 ± 0.08	2.90 ± 0.40	3.24 ± 0.40	6.39 ± 0.57
0.136	0.14 ± 0.08	1.83 ± 0.35	2.52 ± 0.45	4.49 ± 0.58
0.110	0.10 ± 0.07	1.48 ± 0.30	2.43 ± 0.45	4.01 ± 0.55
0.085	0.20 ± 0.10	1.65 ± 0.33	2.61 ± 0.50	4.46 ± 0.60
0.062	0.15 ± 0.08	1.07 ± 0.22	2.81 ± 0.53	4.02 ± 0.58

(18.4 nm), 4p → 2s (11.6 nm), 4d → 2p (13.0 nm), and 4s → 2p (13.2 nm). All the lines are well resolved except the 4s, 4d → 2p lines. From these spectra and the known branching ratios (Klose and Wiese 1989) we have determined the total and partial capture cross sections for the $n=3$ shell, which are collected in table 1 and shown in figure 2 as a function of the impact energy. Errors represent one standard deviation of the statistical uncertainties. All the data have been corrected for the small metastable fraction in the incident O^{6+} beam (5 ± 2%, Mack 1987). These metastables do not interfere with the photon emission measurements but have to be accounted for in the signal normalization. In addition, the $3l$ capture cross sections are corrected for the small (<5%) $n=4 \rightarrow n=3$ cascades.

Concerning the various $4l$ capture cross sections, our measurements show that they are much smaller than 1×10^{-16} cm^2. Unfortunately the present data do not permit a more accurate determination.

3.2. C^{6+} + He

Since the $C^{5+}(nl)$ product states are hydrogenic, the angular momentum states within one n-shell are degenerate. The spectra therefore consist of two peaks in the measured wavelength region: the 3 → 2 line at 18.2 nm and the 4 → 2 line at 13.5 nm. The emission cross sections σ_{em} for the C VI 3 → 2 and 4 → 2 lines as a function of the collision energy are collected in table 2 and shown in figure 3. The full squares in figure 3 represent calculated emission cross sections assuming the same capture cross sections for C^{6+} + He as we measured for the O^{6+} + He system. This and the comparison with the theoretical curves will be discussed in the next section.

4. Discussion

4.1. Classical considerations

Before we compare our experimental results in detail with various close-coupling calculations it is instructive to discuss the gross features of the charge-transfer process

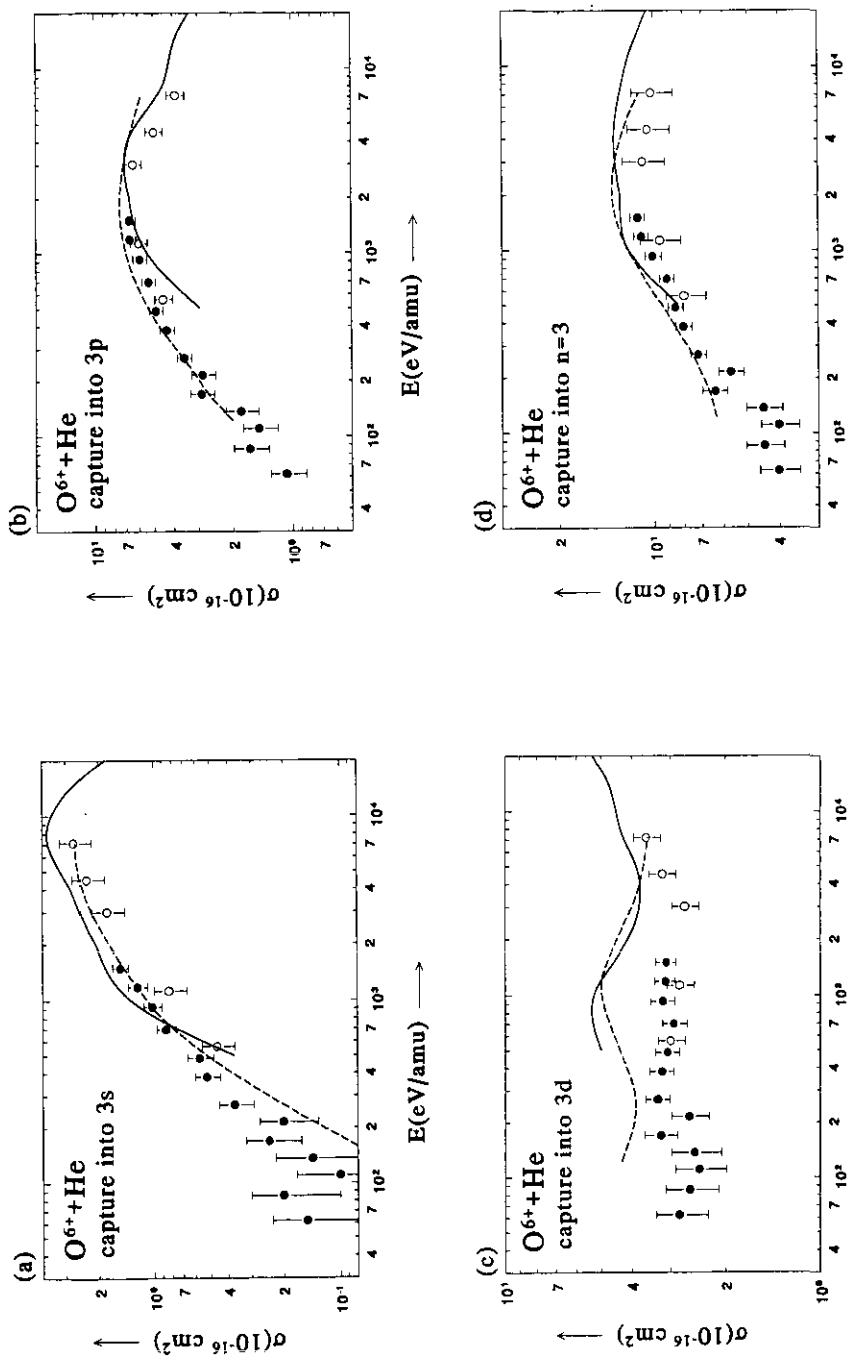

Figure 2. State-selective and total cross sections for single-electron capture into the $n = 3$ shell of O^{5+} during collisions of O^{6+} on He. The error bars represent one standard deviation of the statistical uncertainty. Experiment: ●, this work; ○, Dijkkamp *et al* (1985). Theory: ——, (AO) Fritsch and Lin (1986); - - - -, (MO) Shimakura *et al* (1987). The systematic uncertainty is estimated to be 20%.

Table 2. Measured emission cross sections, σ_{em}, and corresponding statistical errors (in units of 10^{-16} cm^2) for the C VI($3 \rightarrow 2$) and C VI($4 \rightarrow 2$) lines resulting from SEC in C^{6+} + He collisions.

E (keV amu^{-1})	v (au)	$\sigma_{em}(3 \rightarrow 2)$	$\sigma_{em}(4 \rightarrow 2)$
1.852	0.273	5.1 ± 0.8	0.7 ± 0.4
1.136	0.214	3.4 ± 0.5	0.5 ± 0.3
0.805	0.180	3.3 ± 0.5	0.5 ± 0.3
0.595	0.155	2.2 ± 0.5	$0.2^{+0.3}_{-0.2}$
0.403	0.128	2.7 ± 0.6	
0.329	0.115	1.5 ± 0.8	

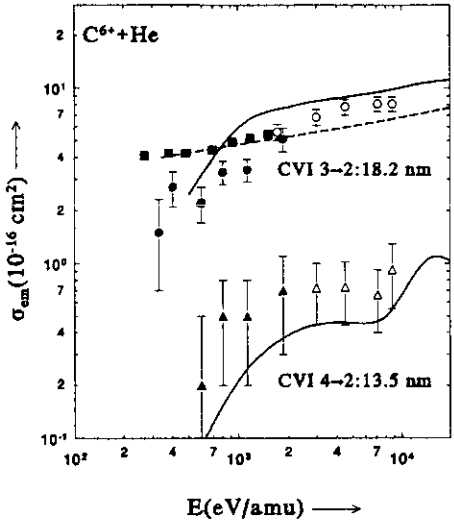

Figure 3. Experimental and theoretical emission cross sections for the C VI $3 \rightarrow 2$ and $4 \rightarrow 2$ lines in collisions of C^{6+} with He. Also shown are the values which are constructed from the experimental $\sigma(3l)$ data for O^{6+} + He collisions. The error bars represent one standard deviation of the statistical uncertainty. The systematic uncertainty is estimated to be 20%. Experiment: ●, ▲, this work; ○, △, Dijkkamp *et al* (1985); ■, constructed from O^{6+} + He data. Theory: ——, (AO) Fritsch and Lin (1986); - - - -, (MO) Kimura and Olson (1984).

in terms of the classical overbarrier model (Ryufuku *et al* 1980). In this model it is assumed that the electron is resonantly transferred from the target atom to the projectile ion when the Coulombic barrier drops below the active electron's binding energy. This happens at an internuclear distance R_{CB} given by

$$R_{CB} = \frac{2q^{1/2}+1}{I_B} \tag{2}$$

with q the charge of the projectile and I_B the ionization potential of the target atom. For the O^{6+}, C^{6+} + He systems R_{CB} equals 6.5 au $= 3.5 \times 10^{-8}$ cm. The total SEC cross section is proportional to the square of R_{CB} and independent of the impact energy. This is in fair agreement with the experimental findings (Iwai *et al* 1982).

Some classical insight into the state-selective SEC cross sections is obtained by comparing the asymptotic binding energy I_q of the electron at the projectile ion, given by

$$I_q = I_B + \frac{q-1}{R_{CB}} \tag{3}$$

with the energy levels of the final product states. This is done in figure 4 where we also show a Gaussian distribution around $I_q = 45.4$ eV (equation (3)) which is related to the time dependence of the potential barrier height (Niehaus 1986). The reaction window shown in the figure is calculated for an impact energy of 0.38 keV amu^{-1}. Figure 4 clearly shows that the more favourable position of the $n = 3$ states relative to the centre of the reaction window compared with the $n = 4$ states explains the predominant population of the former.

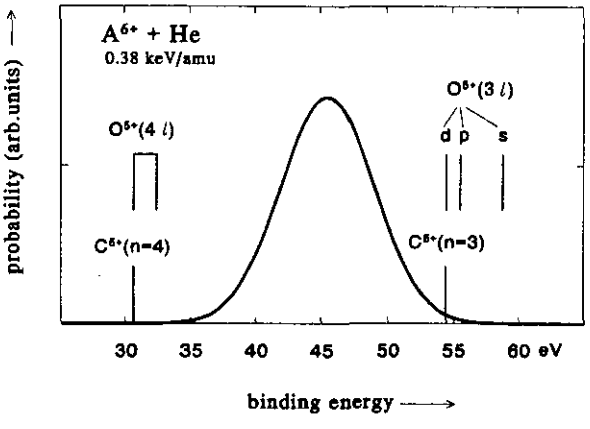

Figure 4. Reaction window for single-electron capture in collisions of C^{6+} and O^{6+} with helium at an impact energy of 0.38 keV amu^{-1}. The positions of the relevant C^{5+} and O^{5+} energy levels are also shown.

Regarding the positions of the $O^{5+}(3l)$ substates relative to the reaction window in figure 4, the classical model predicts for the O^{6+} + He system the $\sigma(3s)$ cross section to be smaller than the $\sigma(3p)$ and $\sigma(3d)$ cross sections. That this is indeed the case can be seen in figure 2.

We finally notice that the various SEC cross sections generally decrease with decreasing impact energy. This is also predicted by the classical model because the width of the reaction window changes proportional to $v^{1/2}$, with v the impact velocity of the projectile ions (Niehaus 1986). However, it is surprising that the $\sigma(3d)$ cross section for the O^{6+} + He system stays fairly constant with decreasing impact velocities: classically speaking the target electron cannot attain angular momenta larger than 0.4 au in the frame of the projectile ion at the lower end of the present energy range (see also Burgdörfer *et al* 1986). It is clear that this effect and the detailed energy dependence of the various cross sections are beyond classical considerations and we have to turn to realistic quantal calculations.

4.2. The O^{6+} + He system

A detailed comparison between experimental SEC cross sections and theoretical models is possible for the O^{6+} + He system because the hydrogenic degeneracy is lifted and

the $O^{5+}(nl)$ product states can easily be resolved spectroscopically (except the 4s and 4d states, see figure 1). Figure 2 shows the various $3l$ SEC cross sections together with the experimental data of Dijkkamp *et al* (1985) and the theoretical calculations of Fritsch and Lin (1986) and Shimakura *et al* (1987). Fritsch and Lin (1986) use an AO expansion suitably extended to (quasi) two-electron systems. Their AO basis consists of one configuration for the He ground state and sixteen configurations representing the He^+ 1s capture product states with the full set of $n = 3, 4$ states of O^{5+}. The electrons of the O^{6+} $1s^2$ core are represented by a model potential. Shimakura *et al* (1987) use a seven-channel MO close-coupling model to calculate the $3l$ SEC cross sections. They represent the O^{6+} $1s^2$ core with a pseudopotential.

As can be seen in figure 2 the two experimental data sets agree with each other in the overlapping energy region and together cover a range of more than two orders of magnitude, e.g. between 0.062 and 7.13 keV amu^{-1}. The AO and MO close-coupling calculations generally reproduce the experimental data fairly well. However, both models overestimate the 3d capture cross section over the entire energy region. It is also interesting to compare the relative populations of the $3l$ states, $\sigma_{rel}(3l) = \sigma(3l)/\Sigma_l\sigma(3l)$, with the theoretical predictions. This is done in figure 5 where the various $\sigma_{rel}(3l)$ are plotted as a function of the impact energy. The scatter in the experimental relative cross sections is reduced significantly because a large contribution to the statistical uncertainty of the absolute cross sections, e.g. the overlap between ion and target beams, is removed in this way. Figure 5 shows that while for the 3s state both the AO and MO models agree excellently with the experimental points, for the 3p and 3d states the MO model reproduces the experimental data better in the low-energy region and the AO model is better in the high energy region. This agrees with the intuitive idea that the MO model is better in describing molecular effects, which become more important at lower impact energies, than the AO model. Notice also that below 200 eV amu^{-1} the 3d state contains more than 50% of the total $n = 3$ population.

4.3. The C^{6+} + He system

The product states after SEC by C^{6+} ions colliding on He are hydrogenic so that the l substates within one n shell are degenerate and cannot easily be resolved. Therefore, we can only determine the emission cross sections for the C VI $3 \rightarrow 2$ line at 18.2 nm and the $4 \rightarrow 2$ line at 13.5 nm. This has been done in the impact energy range between 0.329 and 1.852 keV amu^{-1}. Figure 3 shows our results together with the experimental data of Dijkkamp *et al* (1985) at higher impact energies which join our data points smoothly. The emission cross sections are related to the SEC cross sections via the known branching ratios for hydrogenic states (Bethe and Salpeter 1957). Neglecting capture into $n = 5$ and higher states we find

$$\sigma_{em}(3 \rightarrow 2) = \sigma(3s) + 0.118\sigma(3p) + \sigma(3d) + 0.049\sigma(4s) + 0.042\sigma(4p) + 0.03\sigma(4d) + \sigma(4f) \quad (4)$$

$$\sigma_{em}(4 \rightarrow 2) = 0.584\sigma(4s) + 0.119\sigma(4p) + 0.746\sigma(4d). \quad (5)$$

With these relations we have determined theoretical emission cross sections from published close-coupling models (Fritsch and Lin 1986, Kimura and Olson 1984) which are also shown in figure 3. The AO calculation of Fritsch and Lin (1986) is basically the same as the one for the O^{6+} + He system. Kimura and Olson (1984) performed a

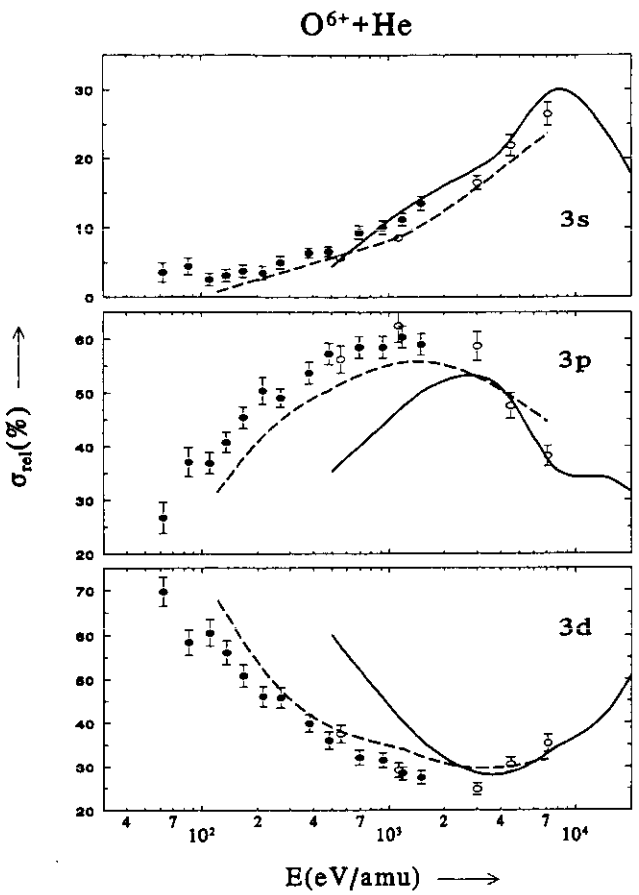

Figure 5. Relative state-selective electron capture cross sections, $\sigma(3l)/\Sigma_l\sigma(3l)$, for O^{6+} colliding with helium. Experiment: ●, this work; ○, Dijkkamp *et al* (1985). Theory: ——, (AO) Fritsch and Lin (1986); - - - -, (MO) Shimakura *et al* (1987).

seven-channel MO close-coupling calculation using molecular $^1\Sigma$, $^1\Pi$ and $^1\Delta$ states which dissociate to the $C^{5+}(n=3)+He^+$ manifold. They neglect capture into the $n=4$ states.

As can be seen from figure 3 both the AO and MO close-coupling calculations describe the experimental data fairly well, although the AO model better reproduces the general trend of both the $3\rightarrow2$ and $4\rightarrow2$ emission cross section as a function of impact energy. This model, however, overestimates $\sigma_{em}(3\rightarrow2)$ particularly around 1 keV amu^{-1}. The MO model fails to reproduce the drop in $\sigma_{em}(3\rightarrow2)$ for impact energies below 1 keV amu^{-1}. One reason for this can be seen by inspecting the $3l$ capture cross sections as calculated with the MO model (Kimura and Olson 1984). This model overestimates capture into the 3d state by at least a factor of two at the lowest energies investigated.

Some information about the $3l$ distribution of the C^{5+*} product ions can be obtained by substituting the measured capture cross sections $\sigma(3l)$ for the $O^{6+}+He$ system into equation (4) (neglecting the very small $n=4$ contributions, e.g. $\ll5\%$) and comparing these emission cross sections with the measured cross sections for $C^{6+}+He$. This is

shown in figure 3 (the squares are the calculated emission cross sections). For impact energies greater than 1.5 keV amu^{-1} the calculated emission cross sections agree with the observed C VI $3 \rightarrow 2$ emission cross sections but they do not show the pronounced drop with decreasing impact energies. One of the reasons for this is that for decreasing impact energies, $\sigma(3d)$ for the $O^{6+}+He$ system stays fairly constant and eventually becomes even larger than $\sigma_{em}(3 \rightarrow 2)$ for $C^{6+}+He$ collisions. We thus conclude that compared with $\sigma(3d)$ for the $O^{6+}+He$ system the 3d capture cross section for $C^{6+}+He$ collisions decreases sharply with decreasing impact energies. This agrees with the $3l$ distribution as calculated with the AO model, see Fritsch and Lin (1986). More detailed information about the 3s and 3p capture cross sections cannot be deduced from this comparison because they do not contribute very much to the $3 \rightarrow 2$ emission cross section. The data shown in figure 3 suggest that for impact energies greater than 1.5 keV amu^{-1} the total $n=3$ capture cross sections are comparable for $C^{6+}+He$ and $O^{6+}+He$ collisions. This might also indicate that the $3l$ distribution is comparable (Gordeev *et al* 1983, Dijkkamp *et al* 1985). However, a definite conclusion cannot be drawn since the $3 \rightarrow 2$ emission cross section is not sensitive for the 3s and 3d ratio.

4.4. Effect of the projectile core on the capture process

As was already noted in the introduction all the previous studies on core effects in SEC relate to collisions between multiply-charged ions and atomic hydrogen. In the following we want to investigate if the core effects as described for these systems are also effective in our case. In particular, Harel and Jouin (1988) found that in collisions of C^{6+} and O^{6+} with H the total cross sections for the dominantly populated $n=4$ states are almost identical for impact velocities larger than 0.3 au. For smaller impact velocities, the $n=4$ capture cross section decreases rapidly for the $C^{6+}+H$ system while it remains more or less constant for $O^{6+}+H$ collisions. In collisions with He the $n=3$ states are dominantly populated and we find the same behaviour for the total $n=3$ capture cross sections as a function of the impact velocity, see section 4.3. The explanation of this phenomenon is well known and discussed in detail in Larsen and Taulbjerg (1984) and Harel and Jouin (1988) for collisions with atomic hydrogen. The general argument is as follows. In real one-electron systems the Coulomb field of the two colliding nuclei exhibits the so-called OEDM (one-electron diatomic molecule) symmetry. As a result there is only one avoided crossing between the initial state and all the final states dissociating to one n shell. When the projectile ion has a core, the OEDM symmetry is broken and the number of avoided crossings is greatly increased. Because charge transfer mainly takes place at these avoided crossings this explains the above-mentioned core effect. We notice that for the $C^{6+}+He$ system the exact OEDM symmetry of the $C^{6+}+H$ system is also broken. Therefore the 'incoming' $4f\sigma$ state also shows avoided crossings with the $3s\sigma$ and $3p\sigma$ states of the $n=3$ manifold just as for the $O^{6+}+H$ system. However, we speculate that for $C^{6+}+He$ collisions the induced splittings will be so small with respect to the strong $4f\sigma$-$3d\sigma$ avoided crossing that the $3s\sigma$ and $3p\sigma$ potential energy curves are always traversed diabatically. Therefore, the same explanation regarding the velocity dependence of the total capture cross sections applies both for H and He targets.

In the previous section we noted that although the total $n=3$ capture cross sections for the C^{6+}, $O^{6+}+He$ collision systems are the same for impact velocities larger than 0.25 au the l distributions need not be identical. Indeed, from theoretical studies Harel and Jouin (1988) find that for C^{6+}, $O^{6+}+H$ collisions the l distributions differ strongly

for $0.3 < v(\text{au}) < 0.6$ and become identical for $v > 0.6$ au. Thus the projectile core does not influence the capture process for $v > 0.6$ au. The l distributions for both collision systems are determined by rotational coupling and the Stark effect caused by the ionized target. For $v < 0.6$ au the Stark effect competes with the projectile core and changes the redistribution of the captured electron over the different l states. The effect of the core is more prominent for the small l states and causes a sharp rise in the 4s population in $O^{6+} + H$ collisions compared with $C^{6+} + H$ for $v < 0.6$ au. We notice that this effect, if present, in collisions with He is masked by the fact that for the $O^{6+} + He$ system the 3s capture cross section is relatively small in this impact velocity range because the $O^{5+}(3s)$ state is situated much further away from the centre of the reaction window compared with the $O^{6+} + H$ system. However, the AO and MO close-coupling calculations of Fritsch and Lin (1986) and Shimakura *et al* (1987) show that qualitatively the picture as described by Harel and Jouin (1988) also applies for the $C^{6+} + He$ and $O^{6+} + He$ collision systems. For example, for $v > 0.7$ au the l distributions are more or less identical, while they differ in the intermediate impact range $(0.25 < v \text{ (au)} < 0.7)$ where the total capture cross sections are still the same. This detailed picture is consistent with the entire experimental data set.

5. Conclusions

In this paper we have studied single-electron capture in collisions of O^{6+} and C^{6+} with He in the impact velocity range between 0.05 and 0.27 au $(62 < E(\text{eV amu}^{-1}) < 1850)$ using photon emission spectroscopy. In both collision systems the $3l$ states are dominantly populated. For the $O^{6+} + He$ system we have determined the l-selective SEC cross sections for the $n = 3$ manifold. Comparing the experimental data with existing AO (Fritsch and Lin 1986) and MO (Shimakura *et al* 1987) close-coupling calculations shows very good agreement for the 3s and 3p states. The 3d capture cross section is overestimated by both models. From the detailed $3l$ distributions we find that the MO model is preferable in the present low-energy regime whereas the AO model seems to reproduce the experimental data of Dijkkamp *et al* (1985) better at higher impact energies.

For the $C^{6+} + He$ system we have measured the C VI $3 \rightarrow 2$ and $4 \rightarrow 2$ emission cross sections. The AO model of Fritsch and Lin (1986) reproduces the experimental data better than the MO model of Kimura and Olson (1984) especially at the lowest impact energies investigated. Finally we have shown that the appealing picture of the influence of the projectile core on the capture process proposed by Harel and Jouin (1988) for collisions of multiply-charged ions with atomic hydrogen also applies for the present O^{6+}, $C^{6+} + He$ collision systems.

Acknowledgments

The authors would like to thank J Eilander and J Sijbring for their excellent technical support. This work is part of the research program of the Stichting voor Fundamenteel Onderzoek der Materie (FOM) with finanical support by the Stichting voor Nederlands Wetenschappelijk Onderzoek (NWO). Via an article 14 contract with JET (Culham, UK) the work is also part of the research programme of the association agreement between FOM and EURATOM with finanical support by NWO.

References

Barat M 1988 *Comment At. Mol. Phys.* **21** 307

Bethe H A and Salpeter E E 1957 *Quantum Mechanics of One- and Two-Electron Atoms* (Berlin: Springer)

Bordenave-Montesquieu A, Benoit-Cattin P, Boudjema M, Gleizes A and Dousson S 1987 *Nucl. Instrum. Methods* B **23** 94

Burgdörfer J, Morgenstern R and Niehaus A 1986 *J. Phys. B: At. Mol. Phys.* **19** L507

Dijkkamp D, Gordeev Yu S, Brazuk A, Drentje A G and de Heer F J 1985 *J. Phys. B: At. Mol. Phys.* **18** 737

Drentje A G 1985 *Nucl. Instrum. Methods* B **9** 526

Fritsch W and Lin C D 1986 *J. Phys. B: At. Mol. Phys.* **19** 2683

—— 1991 *Phys. Rep.* **202** 1

Gordeev Yu S, Dijkkamp D, Drentje A G and de Heer F J 1983 *Phys. Rev. Lett.* **50** 1842

Harel C and Jouin H 1988 *J. Phys. B: At. Mol. Opt. Phys.* **21** 859

Hoekstra R 1990 *Atomic Spectra and Oscillator Strengths for Astrophysics and Fusion Research* ed J E Hansen (Amsterdam: North-Holland)

Hoekstra R, Beijers J P M, Schlatmann A R, Morgenstern R and de Heer F J 1990 *Phys. Rev.* A **41** 4800

Iwai T, Kaneko Y, Kimura M, Kobayashi N, Ohtani S, Okuno K, Takagi S, Tawara H and Tsurubuchi S 1982 *Phys. Rev.* A **26** 105

Janev R K 1991 *Comment At. Mol. Phys.* **26** 83

Kadota K, Dijkkamp D, van der Woude R L, de Boer A, Pan G Y and de Heer F J 1982 *J. Phys. B: At. Mol. Phys.* **15** 3275

Kimura M and Olson R E 1984 *J. Phys. B: At. Mol. Phys.* **17** L713

Klose J Z and Wiese W L 1989 *J. Quant. Spectrosc. Radiat. Transfer* **42** 337

Larsen O G and Taulbjerg K 1984 *J. Phys. B: At. Mol. Phys.* **17** 4523

Liu C J, Dunford R W, Berry H G, Pardo R C, Groeneveld K O, Hass M and Raphaelian M L A 1989 *J. Phys. B: At. Mol. Opt. Phys.* **22** 1217

Mack M 1987 *Nucl. Instrum. Methods* B **23** 74

Mack M and Niehaus A 1987 *Nucl. Instrum. Methhods* B **23** 116

Niehaus A 1986 *J. Phys. B: At. Mol. Phys.* **19** 2925

Okuno K, Tawara H, Iwai T, Kaneko Y, Kimura M, Kobayashi N, Matsumoto A, Ohtani S, Takagi S and Tsurubuchi S 1983 *Phys. Rev.* A **28** 127

Phaneuf R A, Alvarez I, Meyer F W and Crandall D H 1982 *Phys. Rev.* A **26** 1892

Roncin P, Barat M, Gaboriaud M N, Guillemot L and Laurent H 1989 *J. Phys. B: At. Mol. Opt. Phys.* **22** 509

Ryufuku H, Sasaki K and Watanabe T 1980 *Phys. Rev.* A **21** 745

Shimakura N, Sato H, Kimura M and Watanabe T 1987 *J. Phys. B: At. Mol. Phys.* **20** 1801

Taulbjerg K 1986 *J. Phys. B: At. Mol. Phys.* **19** L367